Latest greenhouse product industry in Japan and newest computational techniques for aerodynamics in greenhouses

In-Bok LEE

Laboratory of environmental controls in agricultural buildings
National Research Institute of Agricultural Engineering
Tsukuba, Ibaraki, Japan

Protection agriculture is the essential choice for human to increase the efficiency of limited crop production area under harsh and changeable weather boundary conditions, extend growing season, maximize the crop yields, and then increase the sustainable income of the grower. The investment costs for greenhouses as well as labor and energy costs are much higher than for conventional plant production systems, so these can only be balanced by better crop yields, higher labor productivity, and higher energy efficiency. The protected cultivation in Japan, especially for vegetable productions, has made remarkable progress since the middle of 1970. First of all, this paper introduced the information of general Japanese agriculture and major agricultural productions under cover and in the open according to location, crop types, protected cultivation area, harvested area, and so on. It is the first of a series introducing latest greenhouse product industry in Japan followed by the information of greenhouse types, various environmental control systems in greenhouses, disposals of greenhouse covers, and so on

The second topic in this paper is the newest computational techniques for studying aerodynamics in greenhouses such as computational fluid dynamics (CFD) numerical technique and Particle image velocimetry (PIV) system including large-sized wind tunnel. While directly measuring air velocities and overall natural ventilation rates in multi-span greenhouses is very difficult in full-scaled field experiment, there are much interest recently in CFD and PIV techniques to analyze airflow distributions as well as air quality and thermal

condition in agricultural structures. In this paper, those two newest techniques will be additionally introduced in detail based on the author's on-going researches.

1. Greenhouse product industry in Japan

The total agricultural area in Japan was about 4,718,000ha in 1997, and 13.8%, 0.5%, and 6.4% of the total area were used to produce vegetables, ornamental plants, and fruits, respectively. The cultivated areas of vegetables, ornamental plants, and fruits in the open were 559,300ha, 10,210ha, and 288,900ha, respectively in 1997 while 89,800ha, 10,438ha, and 12,273ha, respectively for protected cultivation. The planted areas of vegetables, ornamental plants, and fruits under cover were 103,622ha, 12,847ha, and 12,459ha, respectively in 1997. In this paper, the protected cultivation includes the uses of greenhouses (glasshouses & plastic houses), rain shelters, and plastic tunnels. Considering the protected and planted areas, the land utilization of glasshouses and plastic houses were 175.5% and 129.9%, respectively.

Table 1 Protected areas for growing vegetables, ornamental plants, and fruit trees in 1999. ( ) indicates the ratio of protected areas for 1999/1991.

	vegetables	**Ornamental plants**	**Fruits**	**Total**
Glasshouse	1,042 ha (20.9%)	1,278 ha (20.3%)	155 ha (-25.5%)	2,475 ha (16.1%)
Plastic house	36,441 ha (7.3%)	7,631 ha (40.9%)	6,969 ha (23.4%)	51,041 ha (13.3%)
Rain shelter	7,012 ha (6.9%)	1,190 ha (42.9%)	5,370 ha (33.7%)	13,572 ha (18.9%)
Plastic tunnel	44,998 ha (-15.2%)	735 ha (26.1%)	0 ha (0.0%)	45,733 ha (-13.3%)
Total	89,493 ha (-5.2%)	10,834 ha (37.3%)	12,494 ha (26.6%)	112,821 (0.6%)

As shown in Table 1, Japan had about 112,821ha of protected cultivation in 1999 while 53,516ha of greenhouse area (glasshouses and plastic houses). The protected cultivation using plastic houses and plastic tunnels were 45.2% and 40.5%, respectively of the total protected area while the use of glasshouses was about 2.2%. Japan is frequently attacked by typhoons every year and has a very hot summer in most areas, so it leads the plastic houses more popular than glasshouses because of cheaper prices and easily rebuilding. This is a sharp contrast with the situation in Holland where glasshouses are mostly used. The table also shows the protected area for ornamental plants greatly increased for last one decade and about 80% of the area were used to produce vegetables. The total protected areas using glasshouses, plastic houses, rain shelters, and plastic tunnels were 2,475ha, 51,041ha, 13,572ha, 45,733ha, respectively, in 1999.

Considering the planted areas of glass & plastic houses in 1999, the major vegetables under cover were tomato (12.8%), normal melon (11.7%), strawberry (11.0%), cucumber (10.6%), Spinach (9.2%), watermelon (7.6%), greenhouse melon (5.7%), eggplants (3.4%), Welsh onion (3.2%), sweet pepper (2.9%), and lettuce (0.8%). While the planted area of ornamental plants under cover was 12,981ha in 1999, the major ornamental plants were chrysanthemum (27.3%), potted flowers (15.3%), rose (5.4%), carnation (5.2%), lily (4.2%), stock (2.4%), and tulip (1.0%). While the planted area of fruit trees was 12,307ha, grapes (54.3%), orange (17.5%), cherry (17.1%), and pear (4.8%) were the major fruits in 1999.

The covering materials used for protected horticulture vary according to the kind of planted crops and their cultivation periods. As shown in Fig 1, the total area of the plastic houses was 51,041ha in 1999 while 2,476ha for glasshouses. It was also shown that the Chloride vinyl films such as Polyvinyl chloride (PVC) and Polyvinyl fluoride (PVF) were the most popular cover materials in Japan, and the use of polyethylene recently increased

significantly. The typical hard plastic films were PET and ETFE while the typical hard plastic panels were fiber reinforced acrylic (FRA), fiber reinforced plastic (FRP), acrylic, and poly-carbonate (PE). Of plastic films, soft ones were used more than hard ones for plastic houses and tunnels. Polyethylene and polyolefin films were usually used as heat insulating materials in plastic houses because the coverings made of these films are easier to open and shut. The structure of glasshouses was mainly steel frames (90% of total), and 83% and 17% of the plastic houses used metal frames and steel frames, respectively.

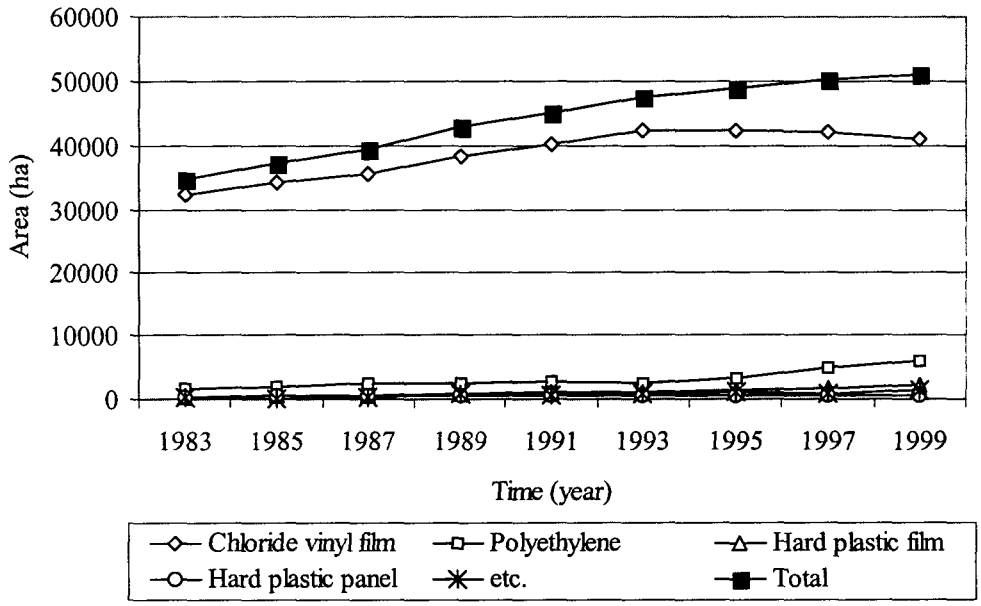

Fig 1 The cover materials of plastic houses when the total area of plastic houses was 51,041ha in 1999.

As I explained above, the main materials were plastic films for plastic houses, tunnels, curtains and mulching. The life of these plastic materials is two to three years and large amount of waster materials is produced every year. Especially noticeable is the increasing

amount of waste PVC and polyethylene films. While the total amount of waste plastics in Japan was 178,887tons in 1999, these films were recycled as construction and agricultural materials (34.8%), disposed to reclaimed land (27.8%) or incinerated (17.6%). The amounts of waste plastics by recycling and dumping to reclaimed land continuously increased, but the amount of incinerated recently decreased significantly because of generating toxic gas when burned.

Table 2 Environmental control systems in greenhouses (glasshouse and plastic houses) in 1999

	Area (ha)	% in total	1999/1995
Heating	23,175	43.3%	111.2%
Controlled Heating	9,792	18.3%	105.6%
Controlled Watering	14,508	27.1%	97.3%
CO2 Supply	856	1.6%	110.0%
Curtained	23,521	43.9%	102.4%
Controlled Vents	5,201	9.7%	124.0%
Natural Venting	43,544	81.4%	102.2%
Forced Venting	9,974	18.6%	118.6%
Soilless culture	1,056	2.0%	194.8%
Total greenhouse Area	53,518	100.0%	104.9%

As shown in Table 2, about 23,000ha of greenhouses (43% of total) was equipped with some apparatus for heating in 1999, and 42% of them were automatically controlled. Many greenhouses also had carbon dioxide generators (1.6%) and internal and external shading curtains (43.9%) to stabilize cultivation and facilitate cultivation work. About 81% of the greenhouses were naturally ventilated in 1999 while about 12% of them had automatically operated vent openings.

Soilless culture has been very attractive as a way to avoid accumulation of salt in soil, occurrence of specific diseases, producing high quality of plants, replanting failure, and saving labor. Additionally, the management of water and nutrients is performed almost automatically and effectively in this culture system. It makes possible high quality of vegetable productions and high yield and income. On the other hand, it requires the construction cost of cultivation facilities, and the cost of electric power and the technical knowledge for their works and maintenance.

Table 3 Area of soilless culture by type in Japan

		1995	1997	1999	1999/1995
Water culture	**DFT**	263	314	313	119.0%
	NFT	99	109	120	121.2%
Solid medium culture	**Gravel**	22	23	25	113.6%
	Sand	6	10	18	300.0%
	Rockwool	139	427	480	345.3%
	Etc.	6	14	60	1000.0%
Spray culture		1	1	10	1000.0%
Etc.		6	18	30	500.0%
Total		542	916	1056	194.8%

While hydroponics, the origin of this culture method, was introduced from 1930s in the U.S., new soilless culture systems were developed using raw materials at around 1970. As shown in Table 3, the total area of soilless culture was 1,056ha in 1999 while the protected area of greenhouses was 53,518ha, and it greatly increased up to about twice of 1995. The major vegetables grown by soilless cultivation were tomato, strawberries, welsh onions, cucumbers, and so on. The area of soilless cultivation for vegetables was 766ha in 1999 while the total soilless cultivation was 1,056ha. Table 3 also indicates an increase of nearly

200% over 1995 for soilless cultivation, and the use of rockwool as a culture medium has been increasing highly. Two typical methods of water culture were nutrient film technique (NFT) and deep flow technique (DFT).

2. Computational techniques for aerodynamics in greenhouses

At National Research Institute of Agricultural Engineering (NRIAE) in Japan, Laboratory of environmental controls in agricultural structures has been investigating the validity of the computational fluid dynamics (CFD, Fluent, Lebanon, NH) model and particle image velocimetry (PIV, TSI Inc., St. Paul, MN, USA) system in studying the natural ventilation characteristics for multi-span greenhouses and evaluating the consequences of various modifications to the natural ventilation systems.

A large-sized wind tunnel system in NRIAE was used for the CFD and PIV validation studies. The wind tunnel offered a rapid, economical, and accurate means for aerodynamic research. With two types of 1/16 scaled multi-span greenhouses (fully open-roof and Venlo-types) built in the wind tunnel, the airflow distributions were computed by PIV system, and then the distributions were compared with the CFD results. PIV, also one of the newest techniques for studying flow fields, simultaneous measures fluid or particle velocity vectors at many points, using optical imaging techniques. Before investigating the CFD validity, the IFA300 Temperature Anemometer sensor (TSI Inc., St. Paul, MN, USA) was used to investigate the PIV validity because only little information of PIV validity were available at the time of this study.

1) Computational fluid dynamics

The CFD technique numerically solves the Reynolds-averaged form of the Navier-Stokes equations within each cell in a domain. The governing equations were discretized on

a curvilinear grid to enable computations in complex and irregular geometry. The Reynolds-averaged process considers the instantaneous fluid velocity to be the sum of a mean and a fluctuating component, the turbulence. Since the high-frequency and small scale fluctuations of turbulent flow can not be directly quantified, turbulence numerical modeling relates some or all of the turbulent velocity fluctuations to the mean flow quantities and their gradients. The governing equations of mass, momentum, and energy used in Fluent are briefly described in Equations (1), (2), and (6), respectively.

$$\frac{\partial \rho}{\partial t} + \frac{\partial}{\partial x_i}(\rho u_i) = 0 \qquad (1)$$

$$\frac{\partial}{\partial t}(\rho u_i) + \frac{\partial}{\partial x_j}(\rho u_i u_j) = -\frac{\partial P}{\partial x_i} + \frac{\partial \tau_{ij}}{\partial x_j} + \rho g_i \qquad (2)$$

where P is the static pressure, τ_{ij} is the viscous stress tensor, and g_i is the gravitational acceleration. μ is the molecular viscosity and the second term on the right hand side is the effect of volume dilation.

$$h = \sum_{i'} m_{i'} h_{i'} \qquad (3)$$

where $$h_{i'} = \int_{T_{ref}}^{T} c_{p,i'} dT \qquad (4)$$

where h is the static enthalpy, T_{ref} is a reference temperature and $C_{p,i'}$ is the specific heat at constant pressure of species i'. It is assumed that diffusion due to pressure and external

forces is negligible. Under this assumption, the energy equation cast in terms of h can be written:

$$\frac{\partial}{\partial t}(\rho h)+\frac{\partial}{\partial x_i}(\rho u_i h)=\frac{\partial}{\partial x_i}\left(k\frac{\partial T}{\partial x_i}\right)-\frac{\partial}{\partial x_i}\sum_{j'}h_{j'}J_{j'}+\frac{\partial P}{\partial T}+u_i\frac{\partial P}{\partial x_i}+\tau_{ij}\frac{\partial u_i}{\partial x_j} \quad (5)$$

where T is the temperature, $J_{j'}$ is the flux of species j', and k is the mixture thermal conductivity.

The turbulent kinetic energy (k) and its rate of dissipation (ε) are obtained from the following transport equations:

$$\rho\frac{Dk}{Dt}=\frac{\partial}{\partial x_i}\left[\left(\mu+\frac{\mu_t}{\sigma_k}\right)\frac{\partial k}{\partial x_i}\right]+G_k+G_b-\rho\varepsilon-Y_M \quad (6)$$

$$\rho\frac{D\varepsilon}{Dt}=\frac{\partial}{\partial x_i}\left[\left(\mu+\frac{\mu_t}{\sigma_\varepsilon}\right)\frac{\partial \varepsilon}{\partial x_i}\right]+C_{1\varepsilon}\frac{\varepsilon}{k}\left(G_k+C_{3\varepsilon}G_b\right)-C_{2\varepsilon}\rho\frac{\varepsilon^2}{k} \quad (7)$$

In these equations, G_k represents the generation of turbulent kinetic energy due to the mean velocity gradients. G_b is the generation of turbulent kinetic energy due to buoyancy. Y_M represents the contribution of the fluctuating dilatation in turbulence to the overall dissipation rate. $C_{1\varepsilon}$ (1.44), $C_{2\varepsilon}$ (1.92), and $C_{3\varepsilon}$ (0.09) are constants. σ_k (1.0) and σ_ε (1.3) are the turbulent Prandtl numbers for k and ε, respectively. The eddy turbulent viscosity, μ_t, is computed by combining k and ε as follows:

$$\mu_t = \rho C_p \frac{k^2}{\varepsilon} \tag{8}$$

2) Large-size wind tunnel system

For last two decades, the large-size wind tunnel system at NRIAE has been used for the experiments of wind loading on the agricultural buildings, airflow and temperature distributions in greenhouses and livestock buildings, and gas/dust control from livestock barns, windbreak planning, and rural environmental designs, etc.

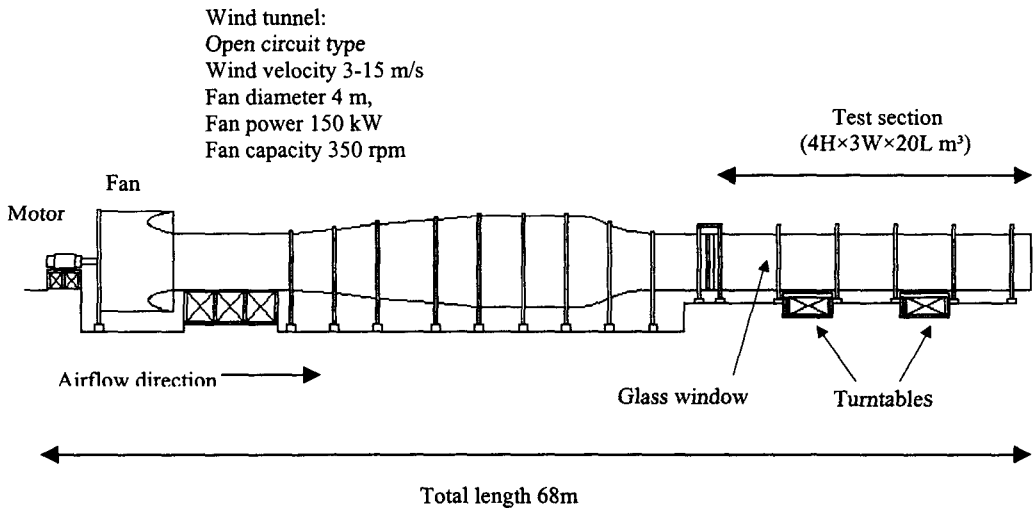

Fig 2 Schematic diagram of large-sized wind tunnel at National Research Institute of Agricultural Engineering in Tsukuba, Japan

As shown in Fig 2, total length of the wind tunnel was 68 m while the size of the test section was 4H×3W×20L (m^3) which had two turntables at the floor. The scaled structures were located on turntables, and the turntables made it easy to investigate the effects of wind

direction by enabling the rotation of the structures. The wind tunnel was an open circuit type, and the minimum and maximum wind velocities simulated in the wind tunnel were 3 m/s and 15 m/s, respectively. The diameter of the fan was 4 m and the maximum rotation capacity and pressure were 350 rpm and 55 mmAq, respectively. Diffusion, strainer, and compression sections made possible to supply uniform and stable airflow into the test section of the wind tunnel. At the test section, the plastic windows on a side wall helped to visually observe and examine the simulated airflows.

The IFA 300 Constant Temperature Anemometer System (TSI Inc., St.Paul, MN, USA) was used to measure the air temperature, 3-dimensional wind velocity and turbulent intensity in the wind tunnel. This system was a fully-integrated, thermal anemometer-based system that measured mean and fluctuating velocity components in airflow fluids. It also measured turbulence and made localized temperature measurements. The system included three-dimensional hot-wired anemometer, thermocouple, data acquisition/analysis software, and A/D converter board. The measuring capacities of the anemometer and thermocouple were 0.1 – 30.0 m/s and 1 – 60 °C, respectively.

3) Particle Image Velocimetry

Fig 3 shows the schematic diagram of the test section of the wind tunnel with Particle Image Velocimetry system. The PIV system includes laser and lightsheet optics, image capture/shifting component, synchronizer, and computer hardware/software.

PIV, by using optical imaging technique, is the simultaneous measurement of fluid or particulate velocity vectors at many points. The measurements were made in planar slices of the flow field while the pulsed laser and the lightsheet optics were part of the illumination system. PIV made fluid velocity measurements by measuring the distance traveled by smoke or particles in the flow in the time between two pulses of light. Double-pulsing the laser gave

two images of each particle in the lightsheet, and the image of the lightsheet created an exposure on the camera. To obtain a flow field image with PIV, the laser pulsed and the CCD video camera was triggered with the correct sequence and timing for the flow conditions. Synchronizer performed this task by controlling the timing of all the components, tying PIV imaging system components together so they functioned as an integrated system. By measuring the distance the particles had moved and dividing the distance by the time elapsed between pulses, the velocity for the particle was determined. By measuring the particle image displacements at many points in the image, the flow field was produced. With velocity measured at high accuracy on a regular grid flow, parameters such as vorticity and strain rates could also be computed.

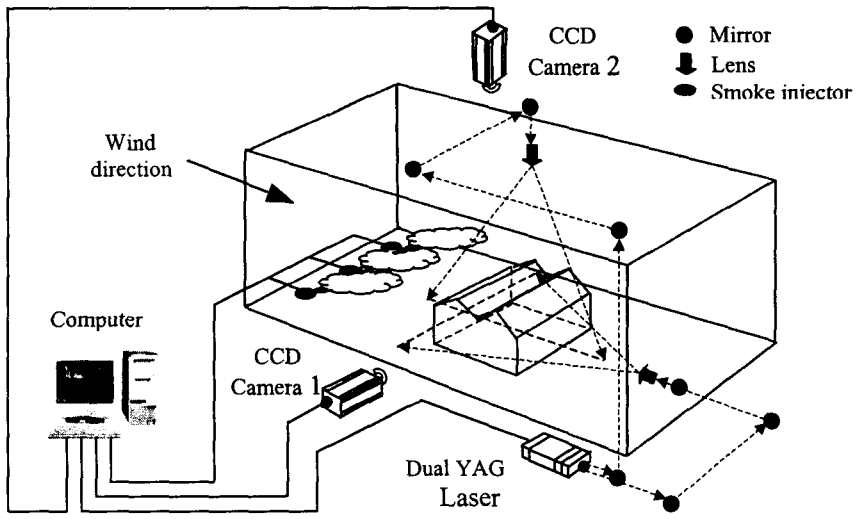

Fig 3 Schematic diagram of the test section of the wind tunnel including Particle Image Velocemetry (PIV) system

In contrast to hotwire or pressure-probe techniques, the PIV is based on the direct determination of the two fundamental dimensions of the velocity: length and time. On the other hand, the technique measures indirectly, because it is the particle velocity which is determined instead of fluid velocity. Therefore, the properties of fluid mechanics for particles must be checked in order to avoid significant discrepancies between fluid motion and particle motion. A primary source of PIV error is the influence of gravitational forces if the density of the fluid ρ and the tracer particles ρ_P do not match. Even if the mismatch in density can be neglected in many practical situations, the gravitationally induced velocity U_g is derived from Stokes drag law in order to introduce the particle's behavior under acceleration. Therefore, spherical particles in a viscous fluid at a very low Reynolds number are assumed. This yields:

$$U_g = d_p^2 \frac{(\rho_P - \rho)}{18\mu} g \qquad (9)$$

where g is the acceleration due to gravity, μ the dynamic viscosity of the fluid, and d_P is the diameter of the particle. In analogy to equation (10), an estimate for the velocity lag of a particle can be derived in a continuously accelerating fluid:

$$U_S = U_P - U = d_P^2 \frac{(\rho_P - \rho)}{18\mu} a \qquad (10)$$

where U_P is the particle velocity. The step response of U_P typically follows an exponential law if the density of the particle is much greater than the fluid density, as shown below:

$$U_P(t) = U\left[1 - \exp\left(-\frac{t}{\tau_S}\right)\right] \qquad (11)$$

with the relaxation time, τ_S, given as follows:

$$\tau_S = d_P^2 \frac{\rho_P}{18\mu} \qquad (12)$$

If the fluid acceleration is not constant or Stokes drag does not apply (e.g. at higher flow velocities) the equations for the particle motion become more difficult to solve, and the solution is no longer a simple exponential decay of the velocity. Nevertheless, τ_S remains a convenient measure for the tendency of particles to attain velocity equilibrium with the fluid.

In this study, the smoke generator (LAS-N TYPE, Seika Co., Osaka, Japan) and air compressor (GK-55 TYPE, MEIJI Air Compressor MFG. Co., Osaka, Japan) were used to make smoke in the airflow in the wind tunnel. The smoke generator used the Dioctyl Sebacate liquid to make smoke, and the maximum working pressure and tank volume of the air compressor were 1.08 MPa and 150 liters, respectively.

The analysis and display components of the PIV system consisted of the Insight software and a Frame Grabber and array processor. Insight software processed the digital PIV images and measured the velocity throughout the flow field. The velocity vectors were displayed as a graphic overlay on top of the image. With post-processing, flow properties like vorticity and strain rate were computed from the processed vector field.